




NIR regeneration and visible luminescence modification in photochromic glass: A novel encryption and 3D optical storage medium

Heping Zhao^{1,2} | Yuewei Li³ | Chao Mi³ | Yingzhu Zi^{1,2} | Xue Bai¹ |
 Asif Ali Haider¹  | Yangke Cun¹ | Anjun Huang¹ | Yue Liu¹ |
 Jianbei Qiu¹ | Zhiguo Song¹ | Jiayan Liao³  | Ji Zhou⁴ | Zhengwen Yang¹ 

¹College of Materials Science and Engineering, Kunming University of Science and Technology, Kunming, People's Republic of China

²Southwest United Graduate School, Kunming, People's Republic of China

³Institute for Biomedical Materials and Devices (IBMD), Faculty of Science, University of Technology Sydney, Sydney, New South Wales, Australia

⁴State Key Lab of New Ceramics and Fine Processing, Department of Materials Science and Engineering, Tsinghua University, Beijing, People's Republic of China

Correspondence

Jiayan Liao, Institute for Biomedical Materials and Devices (IBMD), Faculty of Science, University of Technology Sydney, Sydney, NSW 2007, Australia.
 Email: jiayan.liao@uts.edu.au

Ji Zhou, State Key Lab of New Ceramics and Fine Processing, Department of Materials Science and Engineering, Tsinghua University, Beijing 100084, People's Republic of China.
 Email: zhouji@tsinghua.edu.cn

Zhengwen Yang, College of Materials Science and Engineering, Kunming University of Science and Technology, Kunming 650093, People's Republic of China.
 Email: yangzw@kust.edu.cn

Funding information

Key Project of the National Natural Science Foundation of China-Yunnan Joint Fund, Grant/Award Number: U2102215; National Natural Science Foundation of High End Foreign Expert Introduction Plan, Grant/Award Number: G2022039008L; Academician Workstation of Cherkasova Tatiana in Yunnan Province, Grant/Award Number: 202305 AF150099; Yunnan Province Major Science and Technology Special Plan, Grant/Award Number: 202302AB080005

Abstract

Photochromic glass shows great promise for 3D optical information encryption and storage applications. The formation of Ag nanoclusters by light irradiation has been a significant development in the field of photochromic glass research. However, extending this approach to other metal nanoclusters remains a challenge. In this study, we present a pioneering method for crafting photochromic glass with reliably adjustable dual-mode luminescence in both the NIR and visible spectra. This was achieved by leveraging bimetallic clusters of bismuth, resulting in a distinct and novel photochromic glass. When rare-earth-doped, bismuth-based glass is irradiated with a 473 nm laser, and it undergoes a color transformation from yellow to red, accompanied by visible and broad NIR luminescence. This phenomenon is attributed to the formation of laser-induced (Bi⁺, Bi⁰) nanoclusters. We achieved reversible manipulation of the NIR luminescence of these nanoclusters and visible rare-earth luminescence by alternating exposure to a 473 nm laser and thermal stimulation. Information patterns can be inscribed and erased on a glass surface or in 3D space, and the readout is enabled by modulating visible and NIR luminescence. This study introduces a pioneering strategy for designing photochromic glasses with extensive NIR luminescence and significant potential for applications in high-capacity information encryption, optical data storage, optical communication, and NIR imaging. The exploration of bimetallic cluster formation in Bi represents a vital contribution to the advancement of multifunctional glass systems with augmented optical functionalities and versatile applications.

This is an open access article under the terms of the [Creative Commons Attribution](https://creativecommons.org/licenses/by/4.0/) License, which permits use, distribution and reproduction in any medium, provided the original work is properly cited.

© 2024 The Authors. *InfoMat* published by UESTC and John Wiley & Sons Australia, Ltd.

KEYWORDS

optical storage, photochromic glass, reproducible NIR luminescence

1 | INTRODUCTION

The exponential surge in information data demands advancements in optical storage technologies. A range of strategies, including 3D optical storage media and dual light beam systems, have been explored to enhance data storage density.^{1–6} Photochromism, a phenomenon characterized by color changes induced by light irradiation, has emerged as a promising mechanism for optical storage.^{7,8} However, relying on absorption modulation for optical information readout may result in a high noise ratio, owing to the reduced absorption contrast caused by the photochromic effect.

To overcome this limitation, researchers have investigated photochromic ceramics doped with rare-earth ions as potential optical storage media, achieving a high information readout ability through the reversible modification of the absorption and luminescence states.^{9–13} Transparent glass, which is known for its three-dimensional optical storage capacity, has emerged as an especially promising medium.^{14–18} Recently, a transition from two-dimensional to three-dimensional optical storage modes has been achieved in photochromic glasses doped with rare-earth ions. Notably, the incorporation of W^{6+} valence state changes and silver nanoparticles have been recognized to confer photochromic properties to glass.^{19,20} However, the development of novel photochromic glasses remains challenging. In addition, existing approaches for optical information readout in glass based on the reversible modification of visible luminescence still face challenges in terms of information security.^{21,22} Leveraging NIR luminescence as a controllable readout signal in optical information storage media is promising for bolstering information security. Although studies have been conducted to modulate the NIR luminescence, achieving reversible regulation based on the photochromic effect remains a frontier that requires further exploration.

Luminescent glasses spanning from the visible to NIR luminescence spectra have been extensively used in optical communication, in vivo imaging, photothermal treatment, tumor detection, displays, and laser technologies.^{23–29} The ability to modulate luminescence across this broad range opens up intriguing possibilities for expanding its utility. Through the manipulation of visible and NIR multimodal luminescence, researchers have demonstrated deep-learning decoding and information encryption.^{30–33} In the context of optical information

storage, readout can be accomplished by controlling the wavelength and intensity of visible or NIR luminescence, facilitating wavelength, or intensity multiplexing, thereby enhancing information security.^{34–37} Consequently, the integration of visible and NIR luminescence modulation into a single glass promises novel avenues for advancing optical data storage and information encryption.

In this study, we introduce a novel mechanism that presents an innovative approach to achieve color-changing and dual-mode luminescence modification properties in glass. By harnessing the formation of bimetallic clusters of bismuth, we designed a unique type of photochromic glass that exhibited reversible color changes accompanied by simultaneous visible and broad NIR dual-mode luminescence (Figure 1). In this study, we investigated the optical behavior of rare-earth ion-doped bismuth-based (ER-Bi) glass using 473 nm laser direct writing technology. The optical behavior of ER-Bi glass was systematically investigated. Under irradiation with a 473 nm laser, the glass underwent a color transformation from yellow to red, accompanied by the generation of broad NIR luminescence attributed to the laser-induced formation of (Bi^+, Bi^0) nanoclusters. Furthermore, we achieved the reversible modulation of NIR luminescence from (Bi^+, Bi^0) nanoclusters and visible luminescence from rare-earth ions by alternating 473 nm lasers and thermal stimulation. The capacity to inscribe and erase information patterns on a glass surface or within an arbitrary 3D space, with data readout enabled by modulating the visible and NIR luminescence, demonstrates the potential of this photochromic glass for high-capacity information encryption, 3D optical data storage, and NIR imaging. This work introduces a groundbreaking strategy to address the prevailing challenges in optical storage and encryption as well as paves the way for significant advancements in optical technologies.

2 | RESULTS AND DISCUSSION

Pure bismuth-based glass (Bi-glass) without rare earth ion doping was prepared with a molar composition of $45\%Bi_2O_3-5\%Al_2O_3-16\%PbO-29\%B_2O_3-5\%Sb_2O_3$. No visible luminescence or weak NIR luminescence was observed for the Bi-glass using various light sources (Figure S1A,B). Upon irradiation with a 473 nm laser, a noticeable decrease in transparency was observed in the Bi-glass within the range of 450–900 nm (Figure S2A).

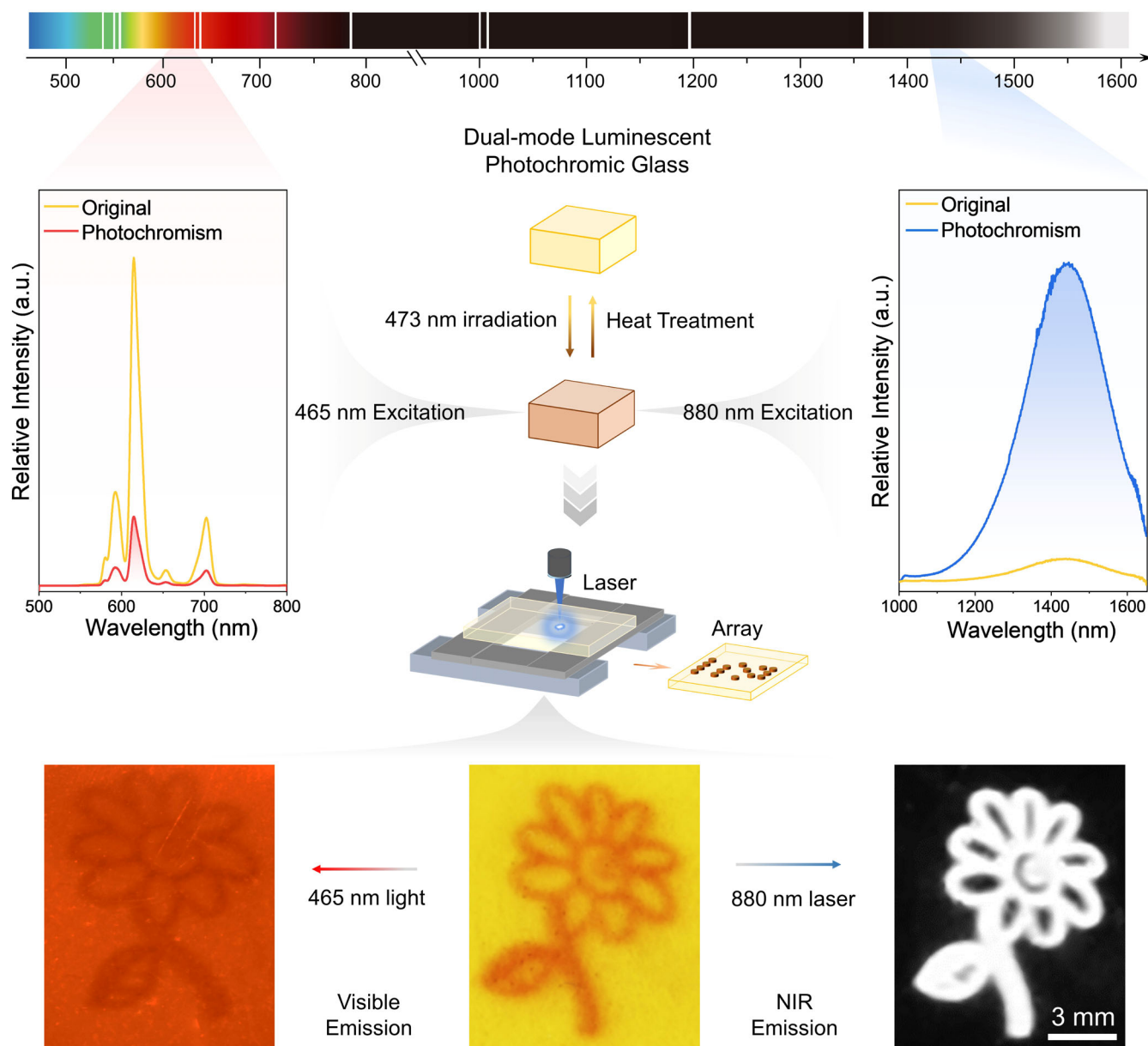


FIGURE 1 Schematic of the 473 nm laser writing system for sample fabrication. Complex photochromic patterns can be controllably created by combining a focused 473 nm laser beam with a 3D XYZ translation stage. Laser induced red coloration in glass can modulate the visible and NIR luminescence intensity, respectively. A 465 nm light from a xenon lamp is used to excite the glass to realize an optical information readout. The white pattern represents NIR luminescence in the photochromic region of the glass upon 880 nm excitation.

This phenomenon indicated a significant photochromic effect, resulting in a color transition from yellow to red. Subsequently, this photochromic glass exhibited intense broad NIR luminescence, peaking at 1450 nm, compared to the raw glass without 473 nm laser irradiation when excited by a 880 nm laser (Figure S2B,C).

To explore the dual-mode luminescence properties in both the visible and NIR regions, various concentrations of Eu^{3+} ions were introduced into the glass. The glass doped with 1 mol% Eu^{3+} , denoted as Eu-Bi, displayed the highest luminescence intensity upon excitation at

465 nm (Figure S3A,B). The doping of Eu^{3+} ions had no significant effect on the transmission of the glass and maintained high transparency (Figure S3C,D). However, no photochromism was observed in the Eu-Bi glass upon irradiation with 365, 808, 880, and 980 nm lasers or with xenon lamp light at 394, 465, and 532 nm. The most prominent color change properties were observed following irradiation with a 473 nm laser (Figure S4). The transparency of the Eu-Bi glass was significantly reduced, saturating within the range of 450–900 nm after irradiation with a 473 nm laser at a power density of

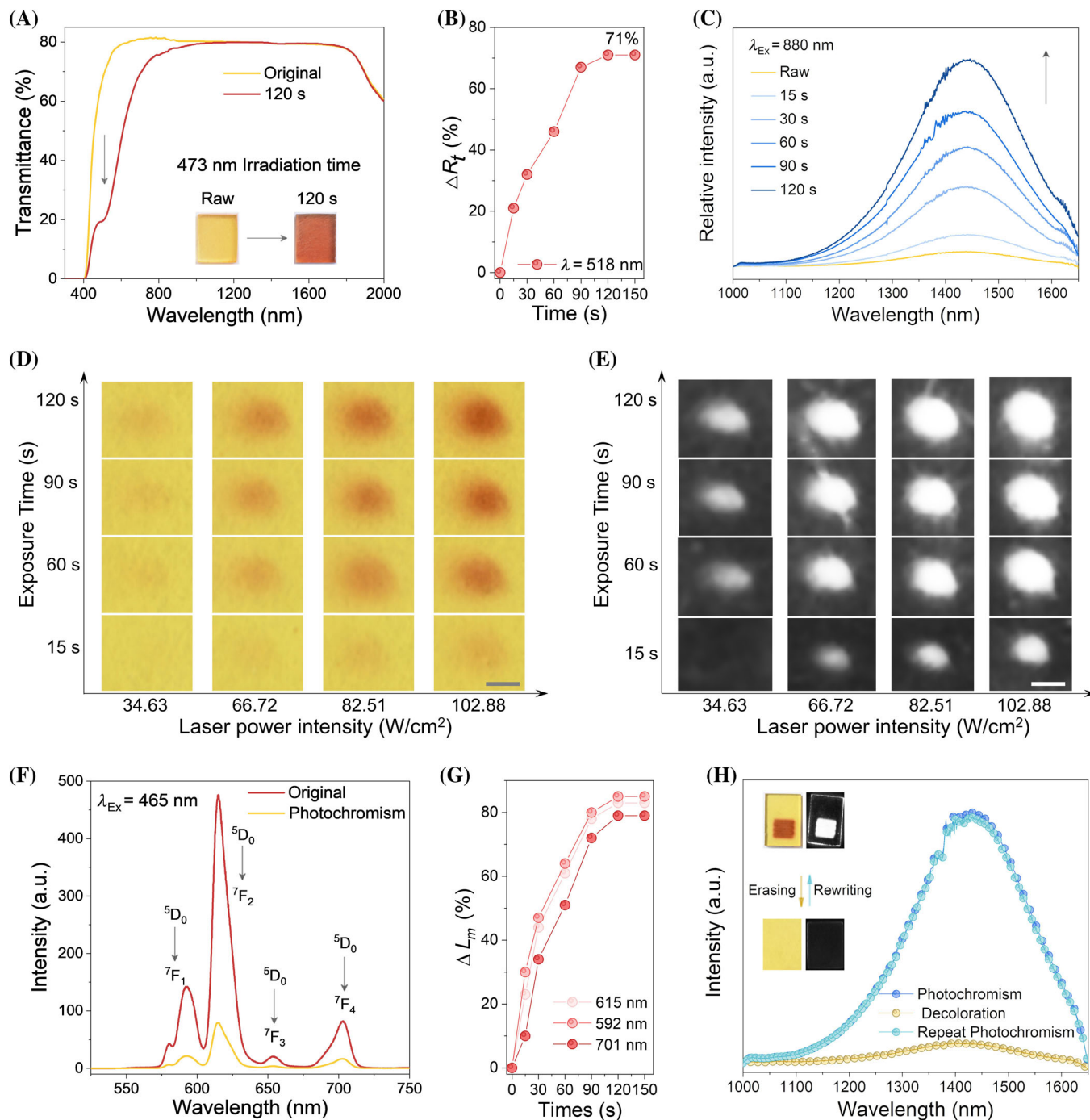


FIGURE 2 Reversible photochromism induced visible and NIR luminescence modification. (A) Transmission spectra and photos of Eu-Bi glass before and after 473 nm laser with 102.88 W cm^{-2} irradiation for 2 min, (B) Corresponding ΔR_t and (C) NIR luminescence spectra under 880 nm laser excitation in Eu-Bi glass after different 473 nm laser irradiation durations. (D) Optical images and (E) NIR luminescent photos under 880 nm laser excitation of Eu-Bi glass after 473 nm laser irradiation with different power densities and exposure times, scale bar, $900 \mu\text{m}$. (F) Modification of luminescence spectra and (G) degrees under 465 nm excitation before and after 2 min 473 nm laser irradiation. (H) NIR luminescence intensity of an erasing-recovery process of Eu-Bi glass under 880 nm excitation alternate 473 nm laser irradiation (102.88 W cm^{-2}) and heat-treated (350°C).

102.88 W cm^{-2} for 2 min (Figure 2A and Figures S5 and S6). The transmittance modification contrast (ΔR_t) at 518 nm was calculated as $\Delta R_t = (T_0 - T_t) / T_0 \times 100\%$, representing the percentage difference between the

transmittance of the unaltered and photochromic Eu-Bi glass subjected to varying durations of irradiation. ΔR_t increased with increasing irradiation time (Figure 2B), ultimately reaching a high coloration contrast of 71%.

The NIR luminescence intensity of the glass exhibited a positive correlation with irradiation time (Figure 2C). The images of the photochromic effect and NIR luminescence were further enhanced as both the irradiation time and power density of the 473 nm laser increased (Figure 2D,E). The photochromic Eu-Bi glass retained stable and robust NIR luminescence performance (Figure S7A,B), with the NIR luminescence intensity demonstrating an increase with the power of the 880 nm laser (Figure S7C,D). The visible luminescence spectra of the Eu-Bi glass were recorded under 465 nm excitation before and after 2 min of 473 nm laser irradiation (Figure 2F and Figure S8), indicating luminescence modification induced by photochromism. The luminescence modulation contrast, ΔL_m , with the formula $\Delta L_m = (L_0 - L_i)/L_0 \times 100\%$, where L_0 is the luminescence intensity of untreated glass, and L_i is that of photochromic glass post 473 nm laser irradiation for different durations. The ΔL_m at 592, 615, and 701 nm increased with the duration of 473 nm laser irradiation (Figure 2G). After an irradiation time of 2 min, a luminescence modulation contrast of 83% was achieved at 615 nm. Concurrently, with increasing laser power density, both the transmittance and luminescence of the Eu^{3+} -doped glass decreased (Figure S9A,B). Conversely, ΔL_m and NIR luminescence intensity showed an increase with rising laser power density (Figure S9C,D). Furthermore, after thermal bleaching, the glass reverted to its original state, exhibiting no red coloration and reduced NIR luminescence under 880 nm laser excitation (Figure 2H). The rewritable NIR luminescence in Eu-Bi glass was demonstrated through eight cycles of erasing recovery, achieved by employing repeated 473 nm laser irradiation and subsequent thermal bleaching (Figure S10).

The influence of reversible photochromism on the luminescence properties of Dy^{3+} - and Sm^{3+} -doped rare-earth ions in glass (Dy-Bi sample with 1 mol% Dy^{3+} and Sm-Bi sample with 1 mol% Sm^{3+}) was further investigated. The transmission spectra of the Dy-Bi and Sm-Bi glasses after 473 nm laser irradiation are shown in Figure S11, revealing a substantial decrease in the transparency between 450 and 900 nm in the glasses. The similar photochromic behavior observed in the ER-Bi glasses and pure Bi glass suggests that doping did not alter the photochromic nature of the glass. The visible luminescence emitted by the Dy-Bi and Sm-Bi glasses exhibited attenuation (Figure 3A,B) following photochromism upon excitation at optimal wavelengths (Figure S12). The Dy-Bi and Sm-Bi photochromic glasses irradiated with a 473 nm laser for 2 min achieved high visible-luminescence regulation contrasts of 85% and 86%, respectively (Figure 3C).

The absorption spectra of the Eu-Bi, Dy-Bi, and Sm-Bi glasses in the NIR region was displayed in Figure 3D. Notably, no absorption peak was observed from 1000 to 1650 nm for the Eu-Bi glass. The shape and intensity of the NIR luminescence spectra in the Eu-Bi glass were similar to those of pure Bi-glass upon 880 nm excitation (Figure S13). However, distinct sharp absorption peaks were evident in the Dy-Bi and Sm-Bi glasses in the range of 1000–1650 nm. Consequently, the absorption of Sm^{3+} and Dy^{3+} ions induced alterations in the NIR luminescence spectra of the photochromic Dy-Bi and Sm-Bi glasses (Figure 3E,F). The NIR luminescence spectra and peak intensities of the Dy-Bi and Sm-Bi glasses exhibited pronounced changes compared to those of the photochromic Bi-glass devoid of rare-earth ions. To demonstrate the regulation of NIR luminescence, flower-shaped information was inscribed in Eu-Bi, Dy-Bi, and Sm-Bi glasses using a focused 473 nm laser, and the information could be retrieved by modulating visible luminescence (Figure 3G). The NIR luminescence appeared darker in the Dy-Bi and Sm-Bi glasses because of the absorption of Dy^{3+} and Sm^{3+} ions in the NIR region, in contrast to the Eu-Bi glass. These findings confirm that the regulation of the visible and NIR luminescence is a shared characteristic of rare-earth-doped Bi-based glasses.

To investigate the bleaching of the photochromic glass, we irradiated it with a 473 nm laser and subsequently subjected it to heat stimulation. The impact of heat treatment on the bleaching of Eu-Bi saturated photochromic bismuth-based glass was explored (Figure S14). Figure S15A illustrates the transmission spectra of the photochromic Eu-Bi glass heat-treated at 350°C for various durations, demonstrating a progressive transition in color from red to yellow, ultimately reverting to its original state after 7 min. The visible luminescence of the Eu-Bi glass gradually increased, and then reverted to its initial state with an extended duration of heat treatment (Figure S15B,C). The NIR luminescence generated by the photochromic glass gradually diminished and became nearly imperceptible after 7 min of thermal stimulation (Figure S15D). The 518 nm transmission and 615 nm visible luminescence spectra of the Eu-Bi glass could be toggled on and off over 10 cycles with high re-writability and re-erasability (Figure 3H and Figure S16). No discernible degradation in transmission and visible/NIR luminescence was noted after multiple cycles, underscoring remarkable reproducibility and reliability while underscoring potential applications in information encryption, optical anti-counterfeiting, imaging, and other domains.

Structural analysis was conducted via Raman and FT-IR spectroscopy of both raw and photochromic glass (Figure S17), unequivocally confirming that the

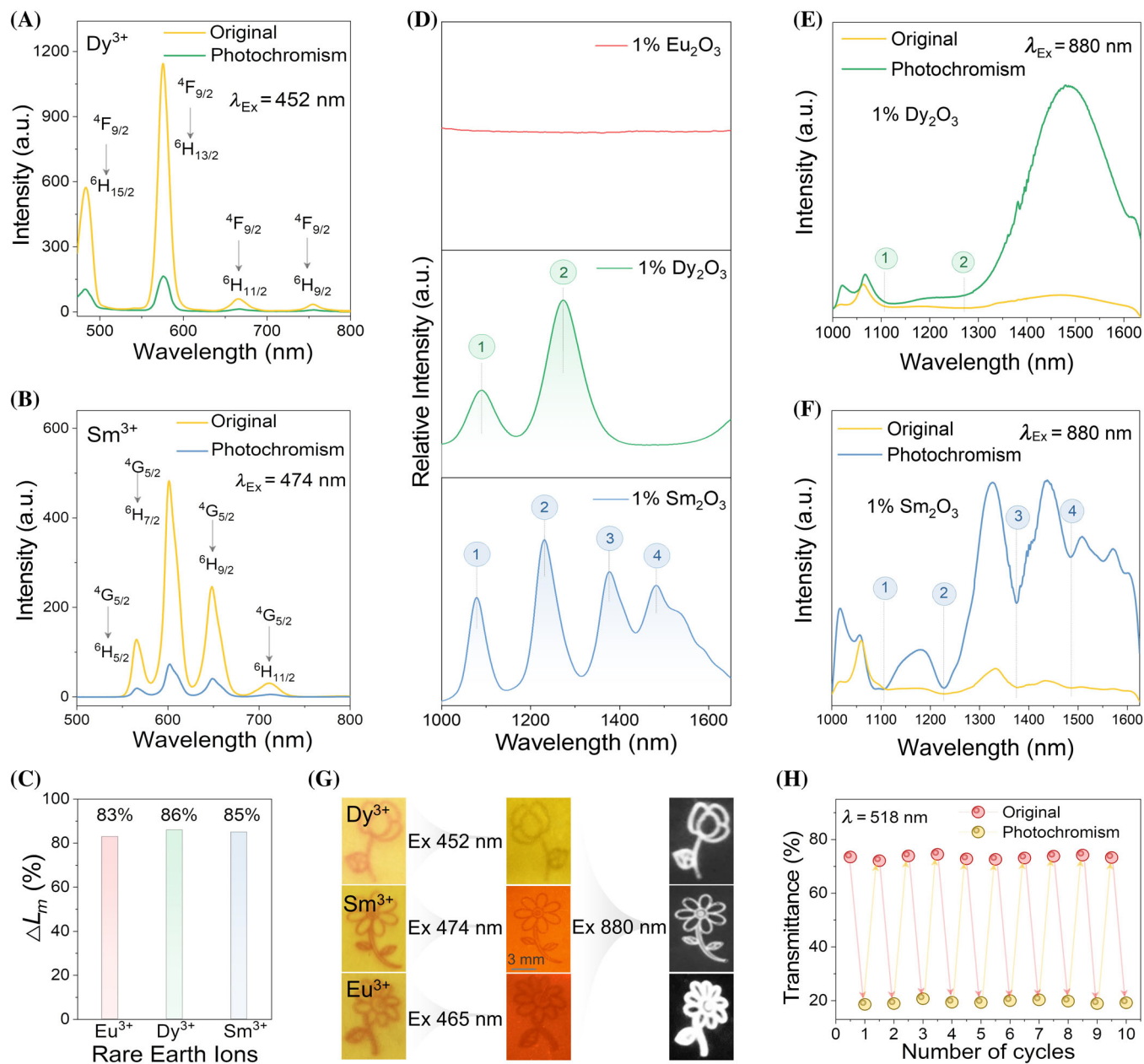


FIGURE 3 Influence of rare earth doping Bi-based glass on optical properties. Visible luminescence spectra of (A) Dy-Bi and (B) Sm-Bi glasses before and after 473 nm laser irradiation for 2 min. (C) Modulation degree of visible luminescence of Eu-Bi (615 nm), Dy-Bi (576 nm), and Sm-Bi (601 nm) photochromic glasses. (D) Absorption spectra of Eu-Bi, Dy-Bi, and Sm-Bi photochromic glasses range from 1000 to 1650 nm. Corresponding NIR luminescence spectra of Dy-Bi (E) and Sm-Bi (F) photochromic glasses. (G) The photochromic pattern, visible, and NIR luminescence pattern of Eu-Bi, Dy-Bi, and Sm-Bi glasses. (H) Transmission intensity at 518 nm of Eu-Bi glass by alternating 473 nm laser (102.88 W cm⁻², 2 min) and thermal stimulation (350°C, 7 min) as a function of cycle numbers.

glass structure remained unaltered after exposure to 473 nm laser irradiation. Furthermore, the photochromism and NIR luminescence observed in the Eu-Bi glass closely mirror those of the Bi glass, suggesting that rare-earth doping does not play a role in the laser-induced effects. Thermoluminescence (TL) analysis (Figure S18) reveals no discernible peaks in the TL curves, effectively excluding the formation of defects, such as oxygen

vacancies as the underlying cause of laser-induced photochromism and NIR luminescence in the glass.

The XPS analyses of Bi and Sb (Figure S19) revealed noteworthy shifts in the binding energies of Bi and alterations in the shape of Sb in the photochromic glass, indicating a change in the valence states of Bi and Sb following 473 nm laser irradiation. Specifically, the XPS spectra of Bi in the raw Eu-Bi glass (Figure 4A) exhibited

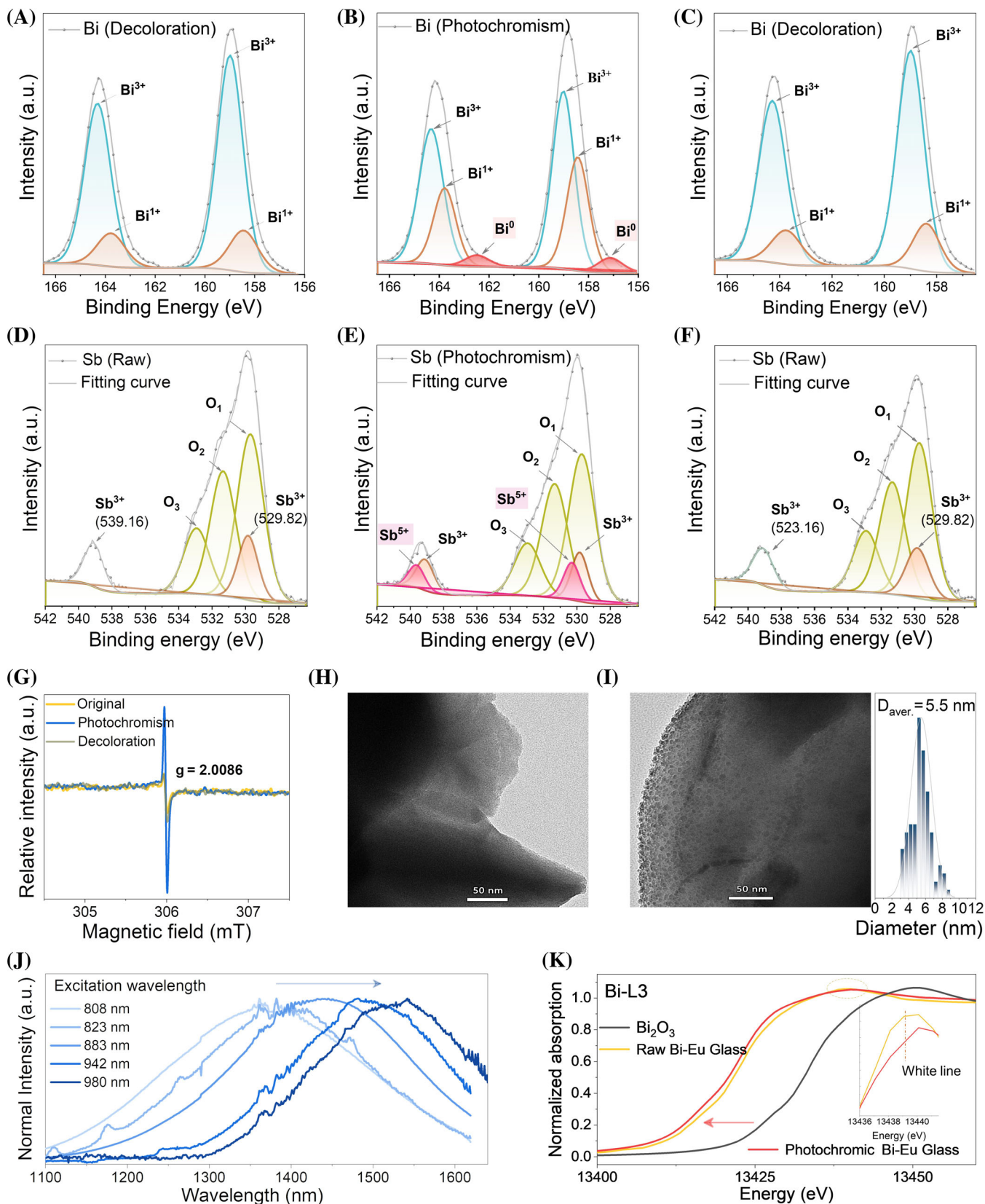


FIGURE 4 Reversible photochromic and reproducible NIR luminescent mechanism. XPS spectra of (A–C) Bi and (D–F) Sb element in Eu-Bi glass before and after photochromism (473 nm laser, 102.88 W cm^{-2}), further bleached through heat-treatment at 350°C for 7 min. (G) room temperature EPR spectra of the raw, photochromic and bleached Eu-Bi glass. TEM image of the raw (H), photochromic (I) Eu-Bi glass. (J) NIR luminescence spectra of the photochromic Eu-Bi glass upon 808, 823, 883, 942, and 980 nm excitation. (K) Bi L-edge XANES spectra of the raw, photochromic Eu-Bi glass, and Bi_2O_3 standard materials.

intense peaks corresponding to Bi^{3+} ions, accompanied by weak peaks corresponding to Bi^{1+} ions. In contrast, after 473 nm laser irradiation, the XPS spectra of the photochromic glass (Figure 4B) reveal an increased intensity of Bi^{1+} ions and the emergence of a peak at 157.0 eV corresponding to Bi^0 , indicative of the transformation from Bi^{3+} ions to low-valence Bi^{1+} and Bi^0 species.

Similarly, the XPS spectra of Sb in the Eu-Bi glass (Figure 4D) indicate the presence of Sb^{3+} ions in the raw Eu-Bi glass, whereas the photochromic Eu-Bi glass (Figure 4E) exhibits distinct peaks corresponding to Sb^{5+} ions after 473 nm laser irradiation. These observations suggest that the reactions induced by 473 nm laser irradiation involve the conversion of $5\text{Sb}^{3+} + 473 \text{ nm } h\nu \rightarrow 5\text{Sb}^{5+} + 10e$ and $4\text{Bi}^{3+} + 10e + 473 \text{ nm } h\nu \rightarrow 2\text{Bi}^{1+} + 2\text{Bi}^0$ in the Eu-Bi glass. XPS spectra of Bi and Sb ions in the bleached glass (350°C for 7 min) (Figure 4C,F) show a decrease in the peaks corresponding to Bi^{1+} ions at 158.47 and 163.78 eV. The XPS peaks corresponding to Sb^{5+} and Bi^0 disappeared. Thermal stimulation may induce reversible reactions in the glass: $2\text{Bi}^{1+} + 2\text{Bi}^0 \rightarrow 4\text{Bi}^{3+} + 10e$ and $5\text{Sb}^{5+} + 10e \rightarrow 5\text{Sb}^{3+}$.³⁸ Consequently, the photochromism was bleached, and the NIR luminescence from the nanoclusters disappeared upon thermal stimulation.

In the electron paramagnetic resonance (EPR) spectra (Figure 4G), a Lorentz line with a g-value of approximately 2.0086 was observed for the raw, photochromic, and decorated glasses, indicating the presence of free electrons from the Bi^{1+} ions. Significantly, the Eu-Bi glass exhibited a robust EPR signal for Bi^{1+} ions after 473 nm laser irradiation.³⁹ This finding strongly suggests that the laser-induced NIR luminescence and photochromism in the Bi glass arise primarily from the formation of low-valence Bi^{1+} and Bi^0 species.

Transmission electron microscopy (TEM) images (Figure 4H,I) reveal the absence of nanoclusters in the raw Eu-Bi glass. However, after 2 min of 473 nm laser stimulation, nanoclusters with a diameter of approximately 5 nm emerged in the photochromic glass. Energy-dispersive x-ray spectroscopy (EDS) of the nanoclusters confirmed the presence of a substantial amount of Bi (Figure S20). The EDS mapping of the original glass (Figure S21) showed a uniform distribution of elements (Bi, Pb, O, Al, Sb, B). After irradiation with a 473 nm laser, the formation of clear nanoparticles was observed, predominantly composed of Bi elements, as revealed by EDS Mapping. This observation indicates that laser irradiation may induce the agglomeration of low-valence Bi^{1+} and Bi^0 species, culminating in the formation of bismuth nanoclusters in photochromic glass.^{40,41} The decay curves of the 1450 nm NIR luminescence illustrate the formation of low-valence Bi^{1+} , Bi^0 , and bismuth clusters

(Figure S22). The NIR luminescence spectra (Figure 4J) revealed a redshift in the luminescence of the photochromic Eu-Bi glass as the excitation wavelength increased. The red photochromic glass exhibiting near-infrared luminescence is due to laser-induced (Bi^{1+} , Bi^0) clusters, including dimers, trimers, tetramers, and so forth, within the bismuth-based glass.⁴²⁻⁴⁴ These Bi clusters, known for their red coloration, contribute to the glass's unique properties.⁴⁵ The formation of (Bi^{1+} , Bi^0) clusters in varying sizes could be associated with a spectrum of energy levels, leading to a redshift in the near-infrared spectrum as the excitation wavelength increases.^{46,47} The valence states of the bismuth ions before and after photochromism were analyzed using Bi L-edge x-ray absorption near edge spectroscopy (XANES), and the intensity of the white line revealed a low average valence state of the Bi ions in the photochromic glass (Figure 4K). These results further demonstrate that the laser-induced NIR luminescence and photochromism in the Eu-Bi glass are primarily attributed to the formation of bismuth nanoclusters.

The radiative transitions of the Eu^{3+} ions from ${}^5\text{D}_0$ to ${}^5\text{F}_n$ ($n = 1, 2, 3,$ and 4) yielded luminescence at 594, 615, 652, and 700 nm, respectively (Figure S23A). The decay curves of the 615 nm luminescence of the Eu-Bi glass following various durations of 473 nm laser irradiation showed minimal changes in the lifetime of the Eu^{3+} ions. This suggests that the luminescence modulation is not caused by the non-resonance energy transfer process (Figure S23B). Notably, the luminescence spectrum of the Eu^{3+} ions overlaps with the absorption band of the photochromic glass (Figure S23C). Moreover, the visible luminescent decay curves of the Dy-Bi and Sm-Bi glasses measured before and after photochromism revealed no significant alteration in the lifetimes of the Dy^{3+} and Sm^{3+} ions (Figure S24). The absorption of the glass host modified the visible luminescence intensity, which increased with longer stimulation times, leading to a greater degree of luminescence modification.

The simultaneous control of rare-earth ions and NIR luminescence provides an opportunity for deep information encryption. Stability tests on data written in photochromic glass under 465 nm light, shown in Figure S25, reveal consistent transmittance spectra and photochromic properties across varying light durations. This confirms the data's stability and allows for nondestructive optical information readout with 465 nm light. Figure 5 illustrates the application of photochromic bismuth glass for reproducible modulation of NIR and visible luminescence. An optical moving platform, controlled by computer software, allows precise control of the 473 nm laser irradiation time on each point of the glass surface (Figure 5A). By reducing the laser spot size (Power: 1712 kW cm^{-2}) and shortening the laser irradiation time to 20 ms, the

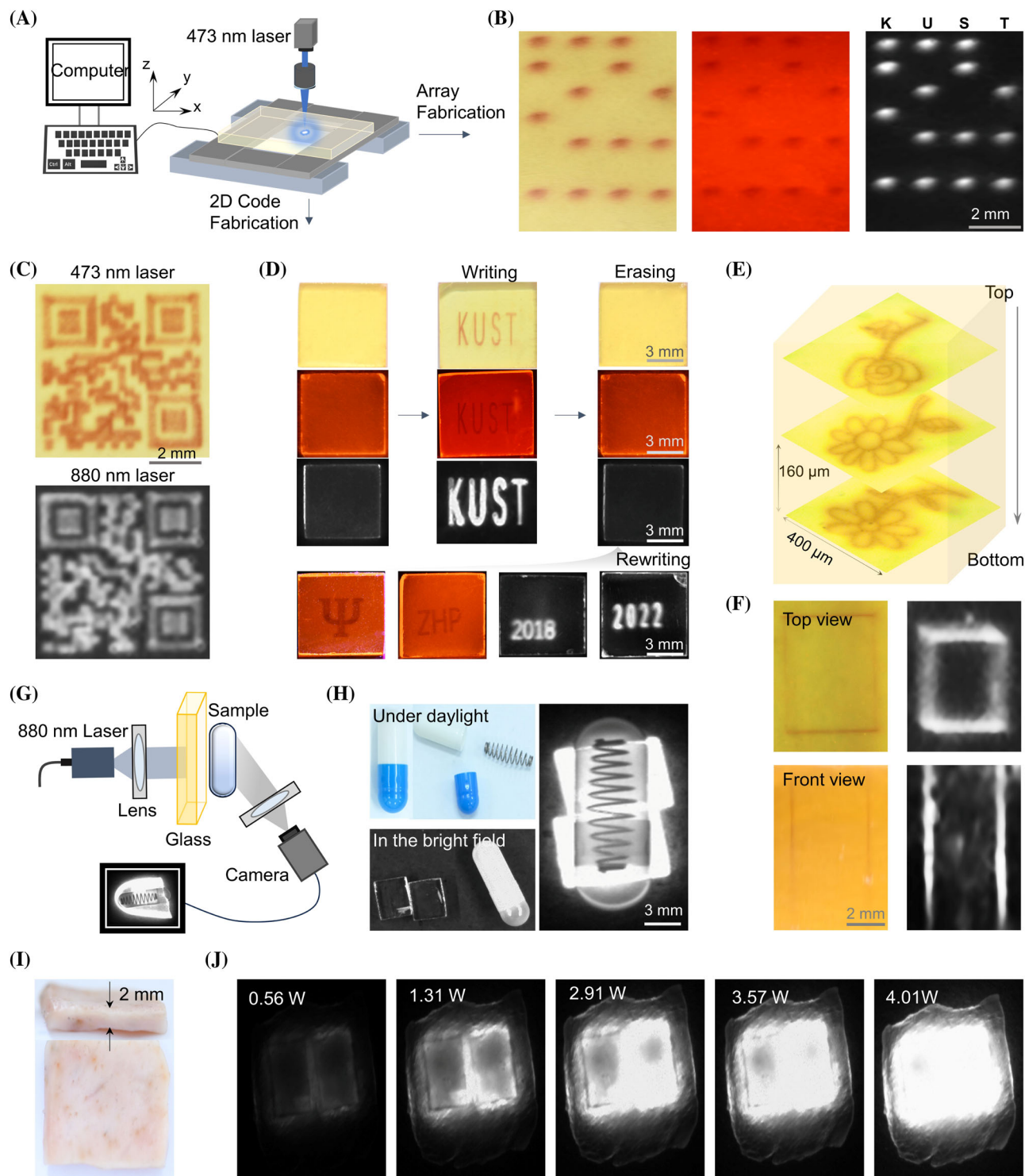


FIGURE 5 Direct lithography of photochromic pattern with 3D optical information storage, encryption, and imaging. (A) Schematic of the 473 nm laser writing system for Eu-Bi glass. (B) The "KUST" alphabet is recorded into the transparent glass by a binary format. Photochromic, visible, and near-infrared luminescence binary pattern. (C) Photochromic two-dimensional code pattern and corresponding NIR luminescent two-dimensional code pattern upon 880 nm laser excitation. The information data are hidden into the photochromic or NIR luminescent two-dimensional code pattern, and the information "KMUST" can be obtained by scanning the two-dimensional code pattern. (D) Writing and recovering the photochromic, visible, and NIR luminescence patterns by alternating 473 nm laser (2 min) and thermal stimulation (7 min). (E) The 3D optical information written in various layers of the glass. (F) The 3D photochromic and NIR luminescence structure inside the glass from the front view and top view. (G) Schematic of the as-designed near-infrared luminescence optical system. (H) Photos of a sample containing a spring in a capsule during the daylight or in the bright field and corresponding imaging photos of the capsule. (I) Photos of real pigskins. (J) Corresponding imaging photos of the pigskins under a 880 nm laser excitation with different laser power.

resolution of the photochromic patterns can be improved to approximately 5 μm (Figure S26A,B). This enables the encoding of binary dot arrays, such as the “KUST” alphabet (Figure 5B), through photochromism-induced luminescence modification upon 465 nm excitation. The binary data can be decrypted using NIR luminescence generated by 473 nm laser irradiation.

More intricate photochromic two-dimensional code (Figure 5C) and school badges (Figure S27) patterns were recorded on the surface of the Eu-Bi glass using laser direct-writing technology. The corresponding NIR luminescence photo of the 2D code can be captured by a near-infrared camera upon 880 nm laser excitation. The optical information “KMUST” can be read out using a smartphone to scan the photochromic or NIR luminescence 2D codes (see Video S1). The photochromic, luminescent, and NIR luminescence patterns could be erased by thermal stimulation, and the recoverability and reversibility of the photochromic glass ensured Eu-Bi glass reuse (Figure 5D). Measurements confirmed the high stability (more than 1 year) of the photochromic pattern protected by the glass matrix (Figure S28). Additionally, complex optical patterns were recorded in various layers of the Bi transparent glass media using laser direct-writing technology (Figure 5E and Video S2). The entire photochromic and NIR luminescent 3D pattern can be processed in the glass interior using focused 473 nm laser irradiation, realizing 3D optical information storage (Figure 5F).

The controllable NIR luminescence of glass is advantageous for night vision security and bioimaging, especially when combined with transparent photochromic glass for display applications. To demonstrate the practicality of photochromic glass with a strong emission for NIR luminescence imaging, a simple NIR imaging system was developed (Figure 5G). The Eu-Bi glass was placed under the target, and the internal structural information of the target was observed through the NIR luminescence generated by laser excitation. Under daylight or bright-field conditions without 880 nm laser excitation, the spring inside the opaque capsule cannot be observed (Figure 5H). However, the contours were clearly visible on NIR luminescence imaging. Similarly, a clear phase contrast of the biological tissue (pigskin tissue) was observed in the NIR luminescence images (Figure 5I). By increasing the excitation power of the 880 nm laser, the infrared luminescence generated by the photochromic glass gradually revealed the structure of the pigskin tissue, demonstrating potential applications in the field of biological imaging.

3 | CONCLUSION

This study presents the direct laser patterning of photochromism and NIR luminescence within transparent glass, leveraging a cost-effective 473 nm semiconductor laser. The dimensions and intensities of the constructed regions were finely tuned by adjusting the laser parameters. Notably, the developed photochromic glasses exhibited exceptional reversibility, reproducibility, and stability, while preserving the strength of the NIR luminescence. By capitalizing on the photochromic effect in rare-earth-doped glass, we achieved the simultaneous modulation of visible and NIR photoluminescence. This breakthrough enabled the encoding and erasure of intricate information patterns in glass, thereby facilitating reversible 3D optical data storage. Through tailored adjustments of the luminescence intensity, optical information can be seamlessly retrieved, promising both high-density storage and enhanced information security. Moreover, the efficacy of 473 nm laser-induced NIR luminescence for biological imaging under 880 nm laser excitation holds substantial promise. This has opened new avenues in the field of biological imaging. Therefore, our study introduced an innovative approach for the concurrent modulation of visible and NIR luminescence in photochromic glass, underscoring its potential applications in 3D optical storage, information encryption, and biological imaging.

AUTHOR CONTRIBUTIONS

Z.Y. and J.L. conceptualized, designed, and oversaw the project. H.Z. executed the experiments with support from J.L. and Z.Y. The manuscript preparation and revisions were collaboratively undertaken by H.Z., J.L., Z.Y., Y.L., and C.M. contributed to the near-infrared luminescence imaging. The entire team engaged in discussions and provided inputs for the manuscript.

ACKNOWLEDGMENTS

This work was supported by the Key Project of the National Natural Science Foundation of China-Yunnan Joint Fund (U2102215), National Natural Science Foundation of High End Foreign Expert Introduction Plan (G2022039008L), Academician Workstation of Cherkasova Tatiana in Yunnan Province (202305 AF150099), and Yunnan Province Major Science and Technology Special Plan (202302AB080005). Thank you for the support provided by the Chancellor's Research Fellowship at the University of Technology Sydney.

CONFLICT OF INTEREST STATEMENT

The authors declare no conflicts of interest.

ORCID

Asif Ali Haider  <https://orcid.org/0000-0001-7020-4111>
 Jiayan Liao  <https://orcid.org/0000-0003-0616-4762>
 Zhengwen Yang  <https://orcid.org/0009-0007-7298-1193>

REFERENCES

- Sun K, Tan D, Fang X, et al. Three-dimensional direct lithography of stable perovskite nanocrystals in glass. *Science*. 2022; 375(6578):307-310.
- Huang XJ, Guo QY, Yang DD, et al. Reversible 3D laser printing of perovskite quantum dots inside a transparent medium. *Nat Photonics*. 2020;14(2):82-88.
- Wiecha PR, Leceste A, Mallet N, Larrieu G. Pushing the limits of optical information storage using deep learning. *Nat Nanotechnol*. 2019;14(3):237-244.
- Parthenopoulos DA, Rentzepis PM. Three-dimensional optical storage memory. *Science*. 1989;245(4920):843-845.
- Dong FL, Chu WG. Multichannel-independent information encoding with optical metasurfaces. *Adv Mater*. 2019;31(45):1804921.
- Wang HT, Wang H, Ruan QF, et al. Coloured vortex beams with incoherent white light illumination. *Nat Nanotechnol*. 2023;18(3):264-272.
- Kobayashi Y, Abe J. Recent advances in low-power-threshold nonlinear photochromic materials. *Chem Soc Rev*. 2022;51(7):2397-2415.
- Ohko Y, Tatsuma T, Fujii T, et al. Multicolour photochromism of TiO₂ films loaded with silver nanoparticles. *Nat Mater*. 2003; 2(1):29-31.
- Yang ZT, Du JR, Martin L, et al. Highly responsive photochromic ceramics for high-contrast rewritable information displays. *Laser Photonics Rev*. 2021;15(4):1804921.
- Ren YT, Yang ZW, Li MJ, et al. Reversible upconversion luminescence modification based on photochromism in BaMgSiO₄: Yb³⁺, Tb³⁺ ceramics for anti-counterfeiting applications. *Adv Opt Mater*. 2019;7(15):1900213.
- Gong J, Du P, Li WP, et al. The enhancement of photochromism and luminescence modulation properties of ferroelectric ceramics via chemical and physical strategies. *Laser Photonics Rev*. 2022;16(10):2200170.
- Jiang T, Zhu YF, Zhang JC, Zhu J, Zhang M, Qiu J. Multistimuli-responsive display materials to encrypt differentiated information in bright and dark fields. *Adv Funct Mater*. 2019;29(51):1906068.
- Li XF, Lin H, Lin SS, et al. Rare-earth-ion doped Bi_{1.5}ZnNb_{1.5}O₇ photochromics: a fast self-recoverable optical storage medium for dynamic anti-counterfeiting with high security. *Laser Photonics Rev*. 2023;17(5):2200734.
- Royon A, Bourhis K, Bellec M, et al. Silver clusters embedded in glass as a perennial high capacity optical recording medium. *Adv Mater*. 2010;22(46):5282-5286.
- Zhang JY, Gecevicius M, Beresna M, et al. Seemingly unlimited lifetime data storage in nanostructured glass. *Phys Rev Lett*. 2014;112(3):033901.
- Tan DZ, Sharafudeen KN, Yue YZ, et al. Femtosecond laser induced phenomena in transparent solid materials: fundamentals and applications. *Prog Mater Sci*. 2016;76:154-228.
- Lin S, Lin H, Ma C, et al. High-security-level multi-dimensional optical storage medium: nanostructured glass embedded with LiGa₅O₈: Mn²⁺ with photostimulated luminescence. *Light: Sci Appl*. 2020;9(1):22.
- Zhang QM, Xia ZL, Cheng YB, et al. High-capacity optical long data memory based on enhanced Young's modulus in nanoplasmonic hybrid glass composites. *Nat Commun*. 2018; 9(1):1183.
- Hu Z, Huang XJ, Yang ZW, et al. Reversible 3D optical data storage and information encryption in photo-modulated transparent glass medium. *Light: Sci Appl*. 2021;10(1):140.
- Zhao HP, Cun YK, Bai X, et al. Entirely reversible photochromic glass with high coloration and luminescence contrast for 3D optical storage. *ACS Energy Lett*. 2022;7(6):2060-2069.
- Xiao DW, Huang XJ, Cun YK, et al. Large reversible upconversion luminescence modification and 3D optical information storage in femtosecond laser irradiation-subjected photochromic glass. *Sci China Mater*. 2022;65(6):1586-1593.
- Li XF, Wu YM, Lin H, et al. Photochromic 3D optical storage: laser-induced regulation of localized optical basicity of glass. *Laser Photonics Rev*. 2023;18(1):2300744.
- Zhou SF, Jiang N, Zhu B, et al. Multifunctional bismuth-doped nanoporous silica glass: from blue-green, orange, red, and white light sources to ultra-broadband infrared amplifiers. *Adv Funct Mater*. 2008;18(9):1407-1413.
- Shi ZG, Lv SC, Tang GW, et al. Multiphase transition toward colorless bismuth-Germanate scintillating glass and fiber for radiation detection. *ACS Appl Mater Interfaces*. 2020;12(15):17764-17771.
- Wang LP, Long NJ, Li LH, et al. Multi-functional bismuth-doped bioglasses: combining bioactivity and photothermal response for bone tumor treatment and tissue repair. *Light: Sci Appl*. 2019;8:52-64.
- Liu XF, Zhou JJ, Zhou SF, et al. Transparent glass-ceramics functionalized by dispersed crystals. *Prog Mater Sci*. 2018;97:38-96.
- Chen SX, Lin JD, Zheng S, et al. Efficient and stable perovskite white light-emitting diodes for backlit display. *Adv Funct Mater*. 2023;33(18):2213442.
- Martyshkin DV, Goldstein JT, Fedorov VV, Mirov SB. Crystal-line Cr²⁺:ZnSe/chalcogenide glass composites as active mid-IR materials. *Opt Lett*. 2011;36(9):1530-1532.
- Ullah I, Rooh G, Khattak SA, et al. Spectral characteristics and energy transfer in Gd³⁺ and Nd³⁺ doped borate glasses for NIR laser applications. *Infrared Phys Technol*. 2022;125:104272.
- Song YP, Lu MY, Mandl GA, et al. Energy migration control of multimodal emissions in an Er³⁺-doped nanostructure for information encryption and deep-learning decoding. *Angew Chem Int Ed*. 2021;60(44):23790-23796.
- Song YP, Lu MY, Xie Y, et al. Deep learning fluorescence imaging of visible to NIR-II based on modulated multimode emissions lanthanide nanocrystals. *Adv Funct Mater*. 2022; 32(45):104272.
- Wang SX, Zhu JW, He YW, et al. Invisible NIR spectral imaging and laser-induced thermal imaging of Na(Nd/Y)F₄@glass with opposite effect for optical security. *Laser Photonics Rev*. 2022;16(8):2200039.

33. Wang WL, Yan S, Liang YJ, et al. A red-light-chargeable near infrared $\text{MgGeO}_3\text{:Mn}^{2+},\text{Yb}^{3+}$ persistent phosphor for bioimaging and optical information storage applications. *Inorg Chem Front*. 2021;8(24):5149-5157.
34. Zhou B, Yan L, Huang JS, et al. NIR II-responsive photon upconversion through energy migration in an ytterbium sublattice. *Nat Photonics*. 2020;14(12):760-766.
35. Gu M, Zhang QM, Lamon S. Nanomaterials for optical data storage. *Nat Rev Mater*. 2016;1(12):16070.
36. Al Sabea H, Norel L, Galangau O, et al. Efficient photomodulation of visible Eu(III) and invisible Yb(III) luminescences using DTE photochromic ligands for optical encryption. *Adv Funct Mater*. 2020;30(30):2002943.
37. Si T, Zhu Q, Zhang T, Sun X, Li JG. Co-doping $\text{Mn}^{2+}/\text{Cr}^{3+}$ in ZnGa_2O_4 to fabricate chameleon-like phosphors for multi-mode dynamic anti-counterfeiting. *Chem Eng J*. 2021;426:131744.
38. Peng MY, Zollfrank C, Wondraczek L. Origin of broad NIR photoluminescence in bismuthate glass and Bi-doped glasses at room temperature. *J Phys Condens Matter*. 2009;21(28):285106.
39. Su LB, Zhao HY, Li HJ, et al. Near-infrared photoluminescence spectra in Bi-doped CsI crystal: evidence for Bi-valence conversions and Bi ion aggregation. *Opt Mater Express*. 2012;2(6):757-764.
40. Wang LP, Cao JK, Lu Y, et al. In situ instant generation of an ultrabroadband near-infrared emission center in bismuth-doped borosilicate glasses via a femtosecond laser. *Photonics Res*. 2019;7(3):300-310.
41. Dianov EM. Bismuth-doped optical fibers: a challenging active medium for near-IR lasers and optical amplifiers. *Light: Sci Appl*. 2012;1(5):e12.
42. Cao JK, Peng J, Wang LP, et al. Broadband NIR emission from multiple Bi centers in nitridated borogermanate glasses via tailoring local glass structure. *J Mater Chem C*. 2019;7(7):2076-2084.
43. Arai Y, Suzuki T, Ohishi Y, Morimoto S, Khonthon S. Ultrabroadband near-infrared emission from a colorless bismuth-doped glass. *Appl Phys Lett*. 2007;90(26):261110.
44. Zhang K, Chen J, Dong Q, et al. Broadband optical amplification in Bi-doped multicomponent glass fiber. *Adv Mater Technol*. 2023;8(12):2202042.
45. Peng M, Qiu J, Chen D, Meng X, Zhu C. Superbroadband 1310 nm emission from bismuth and tantalum codoped germanium oxide glasses. *Opt Lett*. 2005;30(18):2433-2435.
46. Zhang L, Dong G, Wu J, Peng M, Qiu J. Excitation wavelength-dependent near-infrared luminescence from Bi-doped silica glass. *J Alloys Compd*. 2012;531:10-13.
47. Chatterjee J, Chatterjee A, Hazra P. Intrinsic-to-extrinsic emission tuning in luminescent Cu nanoclusters by in situ ligand engineering. *Phys Chem Chem Phys*. 2021;23(45):25850-25865.

SUPPORTING INFORMATION

Additional supporting information can be found online in the Supporting Information section at the end of this article.

How to cite this article: Zhao H, Li Y, Mi C, et al. NIR regeneration and visible luminescence modification in photochromic glass: A novel encryption and 3D optical storage medium. *InfoMat*. 2024;6(9):e12546. doi:10.1002/inf2.12546